51st AIAA/ASME/ASCE/AHS/ASC Structures, Structural Dynamics, and Materials Conference
 18th
12 - 15 April 2010, Orlando, Florida

AIAA 2010-2597

Including Future Tests in the Design of an Integrated Thermal Protection System

Diane Villanueva[1] and Raphael T. Haftka[2], Bhavani V. Sankar[3]
University of Florida, Gainesville, FL, 32611, USA

It is common practice to test components after they are designed. The uncertainty reduction that can occur after a test is usually not incorporated in reliability calculations at the design stage. The reduction in uncertainty is accomplished by the additional knowledge provided by the test and by re-design when the test reveals that the component is unsafe or overly conservative. In this paper, we develop a methodology to estimate the effect of a single future thermal test and model the effect of the resulting uncertainty reduction on the design of an integrated thermal protection system. An integrated thermal protection system protects space vehicles from the severe aerodynamic heating experienced during atmospheric reentry while also functioning as part of the load bearing structure. Using given distributions of computational and experimental errors and given re-design rules, we obtain possible outcomes of the future test through Monte Carlo sampling to determine what changes in probability of failure, design, and weight will occur. In addition, Bayesian updating is used to gain accurate estimates of the probability of failure after a test. We observe that performing a single test can reduce the probability of failure by orders of magnitude, on average, when the objective of re-design is to restore the original safety margins. We show that instead, re-design for a given reduced probability of failure allows additional weight reduction.

Nomenclature

d	=	design variable
Δd_{lim}	=	limit of distance between test design and other design
d_s	=	insulation foam thickness
d_{test}	=	design variable value of test article
e_c	=	computational error
$e_{c,true}$	=	true computational error
e_{extrap}	=	extrapolation error
e_x	=	experimental error
$e_{x,true}$	=	true experimental error
$f_{calc}(T)$	=	probability distribution function of the calculated temperature
$f_{Ptrue}(T)$	=	probability distribution function of the possible true temperature
$f_{test}(T)$	=	probability distribution function of test article temperature
$f_{true}(T)$	=	probability distribution function of true temperature
g	=	limit state function
I	=	indicator function
ini	=	initial
inp	=	input
$l_{test}(T)$	=	likelihood function of obtaining test article temperature
M	=	number of samples of the capacity
m	=	mass per unit area
N	=	number of samples of the response

[1] Graduate Research Assistant, Mechanical & Aerospace Engineering, AIAA Member (dvillanu@gmail.com)
[2] Distinguished Professor, Mechanical & Aerospace Engineering, AIAA Fellow (haftka@ufl.edu)
[3] Ebaugh Professor, Mechanical & Aerospace Engineering, AIAA Associate Fellow (sankar@ufl.edu)

$p_{f,est}$ = estimated probability of failure
$p_{f,true}$ = true probability of failure
$p_{f,est\text{-}corr}$ = test-corrected probability of failure estimate
r = input random variable
r_{test} = random variable value of test article
T_{calc} = calculated temperature
T_{test} = temperature of test article
$T_{test,true}$ = error free test temperature
T_{true} = true temperature
T_{Ptrue} = possible true temperature
T_{meas} = experimentally measured temperature
upd = updated

I. Introduction

In reliability based design optimization, uncertainties are considered when calculating the reliability of the structure. Uncertainty is often compensated for with safety factors and knockdown factors in the design process. However, after design, it is customary for the component to undergo various uncertainty reduction measures (URMs). Examples of URMs in the aerospace field include thermal and structural testing, inspection, health monitoring, maintenance, and improved analysis and failure modeling. Since most components undergo these URMs, it would be beneficial to include their effects in the design process. It would also be beneficial to design the URMs along with the component by optimizing the cost of more weight against the cost of additional tests, redesign, or improved analytical simulations.

This movement to include future tests can be seen in aircraft safety studies by Acar et al[1,2], which investigated the effects of future tests on the final distribution of failure stress and structural design with varying numbers of tests at the coupon, element, and certification levels. Kale et al[3,4] also explored how simultaneous design of the structure and inspection schedule allows the trading of cost of additional structural weight against inspection cost in relation to stiffened panels affected by fatigue crack growth. Studies such as those gave insight into the ability of future tests to reduce uncertainty and thus probability of failure, as well as compare these benefits against the cost of adding more structural weight to dispense with tests.

In this study, we examine the effect of a single future thermal test in the design of an integrated thermal protection system (ITPS) by examining the associated costs along with the resulting change in probability of failure and weight that can result from the test. An integrated thermal protection system protects space vehicles from the severe aerodynamic heating experienced upon atmospheric reentry while also providing some structural load bearing benefit. The thermal test considered in this study measures the maximum temperature of the bottom face sheet, which is critical due to its proximity to the underlying vehicle structure. A design is considered to have failed thermally if it exceeds the maximum allowable temperature.

In previous studies related to the optimization of the ITPS by Kumar et al[5] and Villanueva et al[6], probability of failure calculations considered only the variability in geometric and material parameters and error due to shortcomings in the analytical model. Expanding on those studies, we include the information gained from a test in a temperature estimate, the reduction in uncertainty resulting from the test, and the ability of the test to capture any unexpected behaviors or dangerous designs. Thereby, the objectives of this paper are to (1) present a methodology to both predict and include the effect of a future test, (2) examine the overall changes in design resulting from redesign based on the future test, and (3) illustrate the ability of a test to reduce the probability of failure even when a test shows we are computationally unconservative.

A description of the ITPS is presented in Section II. Next, the uncertainty model and probability of failure calculations are described in Section III. Section IV continues with the methodology to calibrate the computational model based on a test and include redesign based on the test. The method to simulate future tests is summarized in Section V. Section VI presents an illustrative example that details the effect of including the test. The paper then concludes with a summary and ideas for future work in Section VII, and, finally, acknowledgements and references.

II. ITPS Description

Figure 1 shows the ITPS panel being studied, which is a corrugated core sandwich panel concept. The design consists of a top face sheet and webs made of titanium alloy (Ti-6Al-4V), and a bottom face sheet made of

beryllium. Saffil® foam is used as insulation between the webs. The relevant geometric variables of the ITPS design are also shown on the unit cell in Figure 1. These variables are the top face thickness (t_T), bottom face thickness (t_B), thickness of the foam (d_S), web thickness (t_w), corrugation angle (θ), and length of unit cell ($2p$).

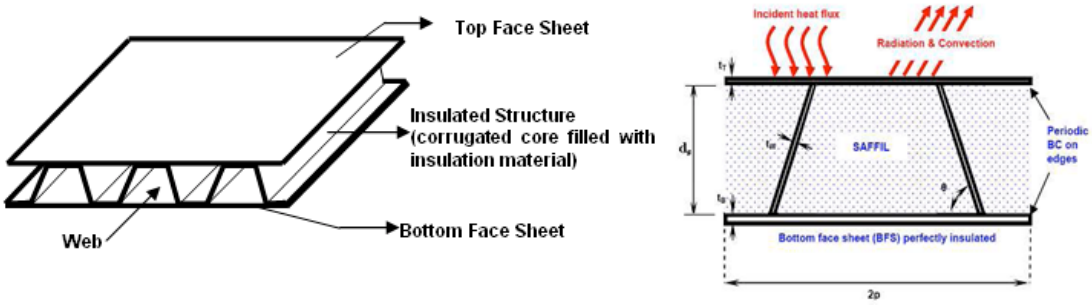

Figure 1. Corrugated core sandwich panel ITPS concept

Thermal analysis of the ITPS is done using 1-D heat transfer equations on a model of the unit cell. The heat flux incident on the top face sheet of the panel is highly dependent on the vehicle shape as well as the vehicle's trajectory. As in previous studies by Bapanapalli[7], incident heat flux on a Space Shuttle-like vehicle was used. A large portion of the heat is radiated out to the ambient by the top face sheet, and the remaining portion is conducted into the ITPS. We consider the worst-case scenario where the bottom face sheet cannot dissipate heat by assuming the bottom face sheet is perfectly insulated. Also, there is no lateral heat flow out of the unit cell, so that heat flux on the unit cell is absorbed by that unit cell only. For a more in-depth description of the model and boundary conditions, the reader is referred to the Bapanapalli reference[7].

The maximum temperature of the bottom face sheet of the ITPS panel is calculated using the quadratic response surface developed by Villanueva et al[5]. It is a function of the previously described geometric variables and the density, thermal conductivity, and specific heat of titanium alloy, beryllium, and Saffil® foam. The mass per unit area m of the ITPS is calculated using Eq.(1), where ρ_T, ρ_B, and ρ_w are the densities of the materials that make up the top face sheet, bottom face sheet, and web, respectively.

$$m = \rho_T t_T + \rho_B t_B + \frac{\rho_w t_w d_s}{p \sin\theta} \tag{1}$$

An experiment that finds the bottom face sheet temperature of a small ITPS panel is usually conducted in a vacuum chamber with heat applied to the top face sheet by heat lamps. The sides of the panel are typically surrounded by some kind of insulation to prevent lateral heat loss. The temperature of the bottom face sheet is found with thermocouples embedded into or in contact with the lower surface of the bottom face sheet.

III. Uncertainty Modeling

A. Classification of Uncertainties

Oberkampf et al[9] provided an analysis of different sources of uncertainty in engineering modeling and simulation, which was further used by Acar et al[1]. We use a similar classification to categorize types of uncertainty as errors (uncertainties that apply equally to each ITPS) or variability (uncertainties that vary in each individual ITPS). We can further describe errors as mostly epistemic and variability as aleatory. It is important to distinguish between types of uncertainty because a specific uncertainty reduction measure may target either error or variability. Tests reduce errors by allowing us to calibrate analytical models. For example, testing can be done to reduce the uncertainty in failure predictions due to high stresses. Variability can be reduced by lowering tolerances in manufacturing. Variability is modeled as random uncertainties that can be modeled probabilistically. In contrast, errors are fixed for a given ITPS and are largely unknown, but here they are modeled probabilistically as well.

Variability in material properties and construction of the ITPS leads to variability in the ITPS thermal response. More specifically, we will have variability in the calculated temperature due to the input variabilities. We simulate this process with a Monte Carlo simulation (MCS) that generates values of the random variables r based on an estimated distribution and calculate the bottom face sheet temperature T_{calc} for each, generating the probability

distribution function. The calculated temperature distribution that reflects the random variability is denoted $f_{calc}(T)$. In estimating the probability of failure, we also need to account for the modeling or computational error. We denote this computational error by e_c, where e_c is modeled as a uniformly distributed random variable within confidence limits in our computational model. Unlike the variability, the error has a single value, and the uncertainty is due to our lack of knowledge.

For a given design given by d and r, the possible true temperature T_{Ptrue} can be found by Eq.(2) in terms of possible computational errors e_c. The sign in front of e_c is negative so a positive error implies a conservative calculation, meaning it overestimates the temperature.

$$T_{Ptrue}(d,r,e_c) = T_{calc}(d,r)(1-e_c) \tag{2}$$

Since the analyst does not know e_c and it is modeled as a random variable, we can form a distribution of the possible true temperature, denoted as $f_{Ptrue}(T)$. Figure 2 illustrates how we arrive at this distribution. The input random variables have initial distributions, denoted as $f_{inp}(r)$, and these random variables, in combination with the design variables, lead to the distribution of the calculated temperature $f_{calc}(T)$. The random computational error is applied, leading to the distribution of the possible true temperature $f_{Ptrue}(T)$, which has a wider distribution than $f_{calc}(T)$.

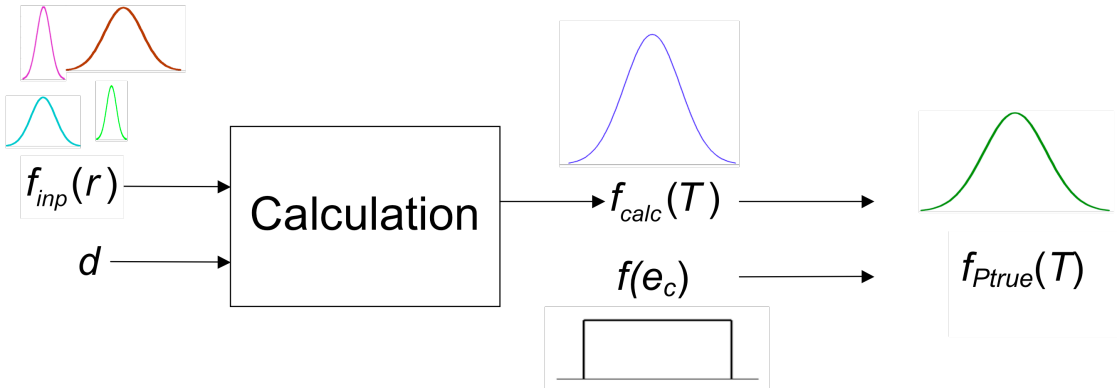

Figure 2. Illustration of the variability of the input random variables, calculated value, computational error, and resulting uncertainty in the estimate

As previously noted, e_c is modeled as a random variable not because it is random, but because its value is unknown. To emphasize this point, the actual true temperature is known only when we know the actual value of e_c as $e_{c,true}$ as illustrated in Eq.(3).

$$T_{true}(d,r) = T_{calc}(d,r)(1-e_{c,true}) \tag{3}$$

Figure 3 shows the probability distribution of the true temperature $f_{true}(T)$, as well as the pdfs of $f_{calc}(T)$ and $f_{Ptrue}(T)$. For this example, we modeled the variability in the material properties, variability in geometry, with normal distributions, and the computational error with a uniform distribution. The plots of each pdf show the probability of exceeding the allowable temperature T_{allow}, represented by the shaded area where the temperature exceeds the allowable. We chose an example where the computational error is unconservative so the $f_{calc}(T)$ provides an underestimate of the probability of failure given by $f_{true}(T)$. This computational error between mean of $f_{calc}(T)$ and the mean of $f_{true}(T)$ is $e_{c,true}$. However, since we include e_c as a random variable, we widened the distribution $f_{calc}(T)$, resulting in $f_{Ptrue}(T)$. This provides a more conservative estimate of the probability that can compensate for the unconservative calculation. Of course, when the error in the calculation is conservative, this wide distribution will grossly overestimate the probability of failure.

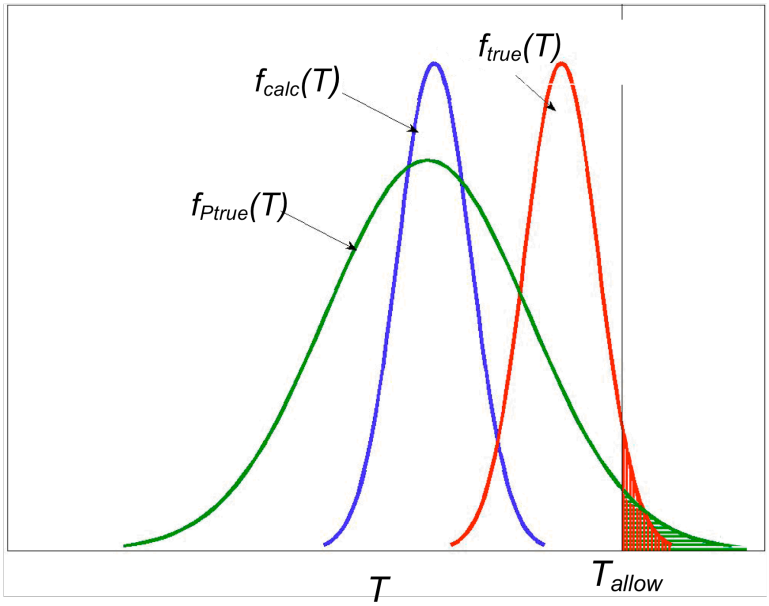

Figure 3. Example with unconservative calculation of temperature showing that including the error in the estimate improves the estimate of the probability of failure

B. True Probability of Failure Calculation

The true probability of failure of a design d with random variables r can be found when the true computational error is known. This is clearly a hypothetical situation, because the true computational error is not known in reality. Here, Monte Carlo simulation (MCS) is used to calculate the true probability of failure. The limit state equation g is formulated as the difference between a capacity C and response R as shown in Eq.(4).

$$g = T_{allow} - T_{true}(d,r) \equiv C - R \tag{4}$$

Since we consider failure to occur when the maximum bottom face sheet temperature exceeds the allowable temperature T_{allow}, the response is T_{true} and the capacity is the allowable temperature. The true probability of failure $p_{f,true}$ is calculated with Eq.(5).

$$p_{f,true} = \frac{1}{N}\sum_{i=1}^{N} I\left[g\left(C_i, R_i\right) < 0\right] \tag{5}$$

The indicator function I equals 1 if the response exceeds the capacity, and equals 0 for the opposite case. The number of samples is N.

C. Estimated Probability of Failure Calculation

Since the true computational error is unknown, the true probability of failure is unknown as well. Instead, we use the calculated temperature T_{calc} and the computational error to determine the estimated probability of failure with the limit state equation formulated as in Eq.(6).

$$g = T_{allow} - T_{calc}(d,r)\left(1 - e_c\right) = C - R \tag{6}$$

Since the two types of uncertainty (computational errors and variability in material properties and geometry) in the response are independent, Separable Monte Carlo[8] (SMC) sampling can be used when evaluating the probability of failure. The limit state equation can be reformulated so that the computational error is on the capacity side, and all random variables associated with material properties and geometry are on the response side.

$$g = \frac{T_{allow}}{1-e_c} - T_{calc}(d,r) \equiv C - R \quad \text{(reformulated)} \tag{7}$$

The estimated probability of failure $p_{f,est}$ can then be calculated with Eq.(8), where M and N are the number of capacity and response samples, respectively. SMC allows for a large number of comparisons between the response and capacity of each limit state, which results in greater accuracy without large computational expense[8]. This is because each response is compared to each capacity in SMC, whereas one response is compared to only one capacity in crude Monte Carlo for the same amount of samples M and N.

$$p_{f,est} = \frac{1}{MN}\sum_{i=1}^{N}\sum_{j=1}^{M} I\left[g\left(C_j, R_i\right) < 0\right] \tag{8}$$

IV. Including the Effect of a Calibration Test

We consider a test, performed for the purpose of validating and calibrating a model for a selected design d_{test} to determine the temperature of the test article T_{test}. We can further assume that the test article is carefully measured for both d_{test} and r_{test}. If no errors are made in the measurements of d_{test}, r_{test}, and T_{test}, then the experimental result is actually the true temperature of the test article. We denote this error-free test temperature $T_{test,true}$..

$$T_{test,true} = T_{true}(d_{test}, r_{test}) \tag{9}$$

However, because of the measurement error, the measured temperature T_{meas} includes the experimental error $e_{x,true}$.

$$T_{meas} = \frac{T_{test,true}}{1-e_{x,true}} \tag{10}$$

Using the computational and experimental results, along with the corresponding error estimates for the test article, we are able to refine the calculated value and its error for any design described by the design variables d and random variables r. In this way, the result of the single test can be used to calibrate calculations for other designs. We examine two methods, which take different approaches in using the test as calibration. The first approach introduces a simple correction factor based on the test result. The second uses the Bayesian method to update the uncertainty of the calculated value for d_{test} based on the test result and then transfers this updated uncertainty to other calculations as the means of calibration.

A. Correction Factor Approach

The correction factor approach is a fairly straightforward method of calibration. Taking advantage of the assumption that the test result is more accurate than the calculated result for the test article, we can scale T_{calc} for any value of d and r by the ratio of the test result to the calculated result to obtain the corrected calculation $T_{calc,corr}$.

$$T_{calc,corr}(d,r) = T_{calc}(d,r)\left(\frac{T_{meas}}{T_{calc}(d_{test}, r_{test})}\right) \tag{11}$$

B. Bayesian Updating Approach

The Bayesian approach uses the experimental result to update the distribution of the temperature of the test article described by d_{test} and r_{test}. From this updated temperature distribution of the test article, we obtain an updated computational error. In this formulation, the probability distribution of the temperature of the test article $f_{test}(T)$ is updated as

$$f_{test}^{upd}(T) = \frac{l_{test}(T) f_{test}^{ini}(T)}{\int_{-\infty}^{\infty} l_{test}(T) f_{test}^{ini}(T)\, dT} \tag{12}$$

where $f_{test}^{ini}(T)$ is the initial probability distribution of the test article's temperature based on $T_{calc}(d_{test}, r_{test})$ and the computational error. The likelihood function $l_{test}(T)$ is the conditional probability density of obtaining the test result T_{meas} given the temperature of the test article.

Once the updated estimate $f_{test}^{upd}(T)$ is known, the Bayesian estimate of the computational error e_{Bayes} can be found with Eq.(3)., where the value of the temperature of the test article T_{test} is obtained from the final distribution $f_{test}^{upd}(T)$.

$$e_{Bayes} = 1 - \frac{T_{test}}{T_{calc}(d_{test}, r_{test})} \tag{13}$$

Therefore, we can replace the possible true temperature given by Eq.(2) with one that uses the Bayesian estimate of the error.

$$T_{Ptrue}(d, r, e_{Bayes}) = T_{calc}(d, r)\left(1 - e_{Bayes}\right)\left(1 - e_{extrap}\right) \tag{14}$$

The additional error e_{extrap} is included to account for the error that occurs when applying this Bayesian estimate of the error to some design other than the test design. This extrapolation error is further described in sub-section 2.

1. Illustrative Example of Calibration by Bayesian Approach

To illustrate how Bayesian updating is used to calibrate calculations based on a single future test, we consider a simple case where both the computational and experimental errors are uniformly distributed. To simplify the problem, we normalize all temperatures by the calculated temperature so that $T_{calc}(d_{test}, r_{test}) = 1$. The error bound of the calculation is ±10% and the error bound of the test is ±7%. The normalized test result is $T_{meas} = 1.05$. The initial probability distribution $f_{test}^{ini}(T)$ and the likelihood function $l_{test}(T)$ are described by Eqs. (15) and (16), respectively.

$$f_{test}^{ini}(T) = \begin{cases} \dfrac{1}{0.2 T_{calc}(d_{test}, r_{test})} & \text{if } \left| \dfrac{T}{T_{calc}(d_{test}, r_{test})} - 1 \right| \le 0.1 \\ 0 & \text{otherwise} \end{cases} \tag{15}$$

$$l_{test}(T) = \begin{cases} \dfrac{1}{0.14 T_{meas}} & \text{if } \left| \dfrac{T - T_{meas}}{T_{calc}(d_{test}, r_{test})} \right| \le 0.07 \\ 0 & \text{otherwise} \end{cases} \tag{16}$$

Since $T_{calc}(d_{test}) = 1$ and the computation error bounds are ±10%, the initial distribution of the true temperature is $f_{test}^{ini}(T) = 5$ on the interval (0.9, 1.1) and zero elsewhere. This is shown in Fig. 4. The test result of $T_{meas} = 1.05$ results in a likelihood of $l_{test}(T) = 1/6.8$ on the interval (0.98, 1.12) and zero elsewhere. Equation (12) is used to find the updated T_{true} distribution so that $f_{test}^{upd}(T) = 8.1$ on the interval (0.98, 1.1) and zero elsewhere.

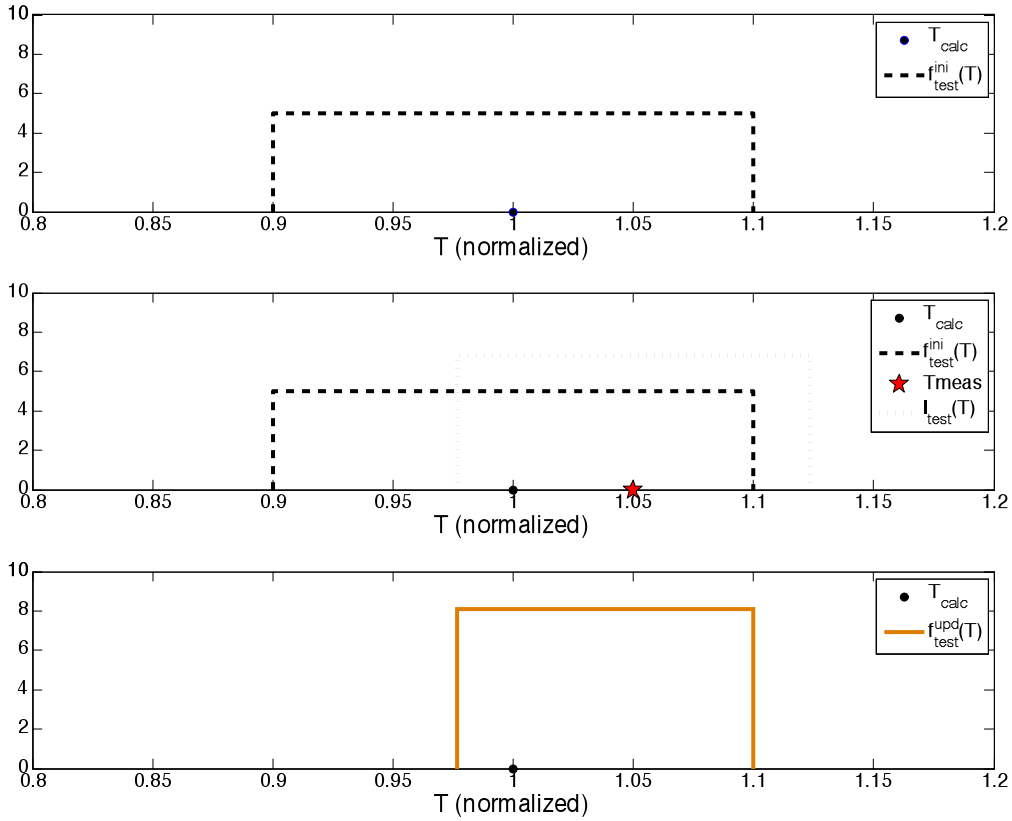

Figure 4. Illustrative example of Bayesian updating showing the initial distribution (top), initial distribution and test (middle), and updated distribution (bottom).

The updated distribution shows that the true temperature is somewhere on the interval (0.98, 1.1). Using this temperature distribution along with the calculated value $T_{calc}(d_{test})$, the updated error distribution e_{Bayes} can be found. Through Eq.(13), we determine that e_{Bayes} is uniformly distributed from -10% to 2.35%.

2. Extrapolation Error in Calibration

Figure 5 illustrates how the Bayesian approach is used to calibrate the calculations for other designs described by d. Here we consider the case when the calculated temperature is linear in the design variable d, and there is no variability (random variables fixed at nominal values).

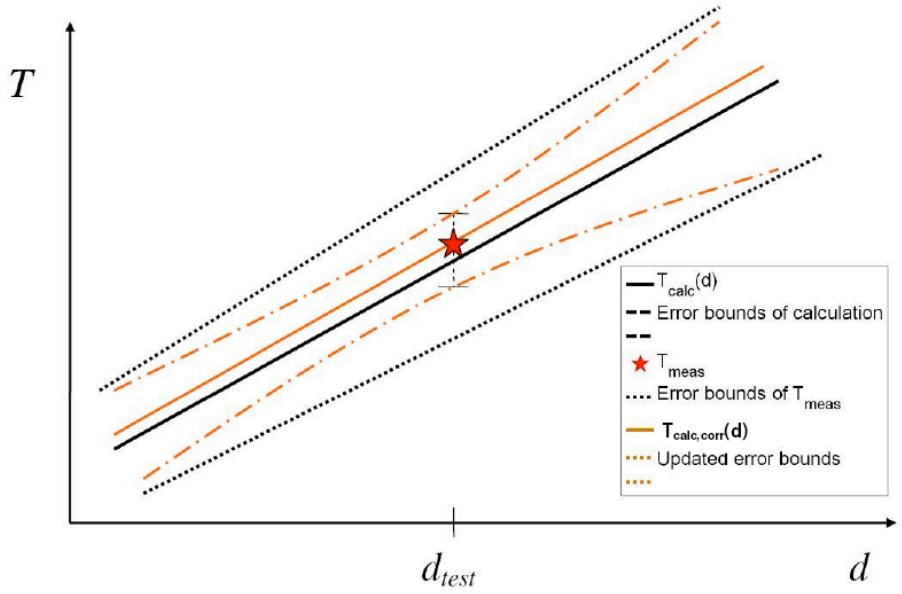

Figure 5. Illustration of the calibration using Bayesian updating

At design d_{test}, we have the same error scenario similar to that illustrated in Figure 4. That is, we represent the calculated temperature at d_{test} as a point on the solid black line, and the error bounds about this calculation by the dotted black lines. The red star represents the experimentally measured temperature, and the error bars show the uncertainty in this temperature. By the Bayesian approach, we obtain a corrected calculated temperature as represented by the point on the orange line (in this situation, this point is the same as the measure temperature), as well as updated error bounds represented by the dashed orange line.

However, this correction and updated error is most accurate at the test design. Therefore, we apply an additional error, the extrapolation error e_{extrap}, when calibrating designs other than d_{test}. Note that at d_{test} the updated error bounds in Figure 5 coincide with the error bounds of the test. As the design becomes increasingly different from d_{test}, the updated error bounds become wider.

The magnitude of e_{extrap} can be determined by the distance between d and d_{test}, such that

$$e_{extrap} = \left(e_{extrap}\right)_{\max} \frac{\left|d - d_{test}\right|}{\Delta d_{\lim}} \tag{17}$$

This defines the extrapolation error so that it is maximum when the distance between d and d_{test} is at limit of this distance $\Delta d_{\lim}$ and zero at the test design.

C. Test-corrected Probability of Failure Estimate

The corrected probability of failure $p_{f,est\text{-}corr}$ after the test can be estimated using the updated error obtained from the Bayesian approach. Separable Monte Carlo is used to calculate $p_{f,est\text{-}corr}$.

$$g = \frac{T_{allow}}{1 - e_{Bayes}} - T_{calc}(d,r)\left(1 - e_{extrap}\right) = C - R \tag{18}$$

$$p_{f,est-corr} = \frac{1}{MN}\sum_{i=1}^{N}\sum_{j=1}^{M} I\left[g\left(C_j, R_i\right) < 0\right] \tag{19}$$

D. Redesign Based on Test

Two criteria for redesign are considered, each with different perspectives on the purpose of the redesign. The first is based on the agreement between the measured value and the calculated value for the test article and the second considers the estimated probability of failure.

1. *Deterministic Redesign*

In deterministic redesign, redesign occurs when there is a significant difference between the experimentally measured temperature T_{meas} and the expected temperature given by the computational model. It is assumed that the temperature given by the computational model (T_{calc}) is the desired value. Therefore, the component is redesigned to restore this original temperature.

The deterministic redesign criterion is implemented by imposing limits on the acceptable ratio on the limits of the measured temperature to the calculated temperature. Redesign occurs when $T_{meas}/T_{calc}(d_{test},r_{test})$ is less than the lower limit D_L (conservative computational model) and or exceeds the upper limit D_U (unconservative computational model).

2. *Probabilistic Redesign*

In probabilistic redesign, the original structure is designed for a specified probability of failure, and redesign is also done to achieve a specified probability of failure. It is reasonable to select the target redesign probability $p_{f,target}$ to be the same as that obtained with probabilistic design. Therefore, redesign occurs when the test corrected probability of failure estimate, given by Eq.(19) is outside the limits of the acceptable range. The lower limit of this range is denoted P_L, and the upper limit P_U.

V. Monte Carlo Simulations to Simulate a Future Test

Monte Carlo simulations are used to simulate the effect of a future test for a design described by design variables d and random variables r with the goal of simulating multiple possible outcomes of this test. To simulate a single outcome of the future test, we first obtain a single sample of the true computational and experimental errors.

Using the calculated value for the test design and the true computational error, we can obtain the true temperature by Eq.(3). Next, the experimentally measured temperature is found using Eq.(10). The choice can be made to calibrate by the correction factor approach or the Bayesian updating approach, and, further, the choice of deterministic or probabilistic redesign can be made.

The true and estimated probabilities of failure after the test can then be determined. At this point, the effect of only one possible outcome of the test has been examined. The major processes involved in the simulation of a single outcome of the test are summarized in the flow chart in Figure 6.

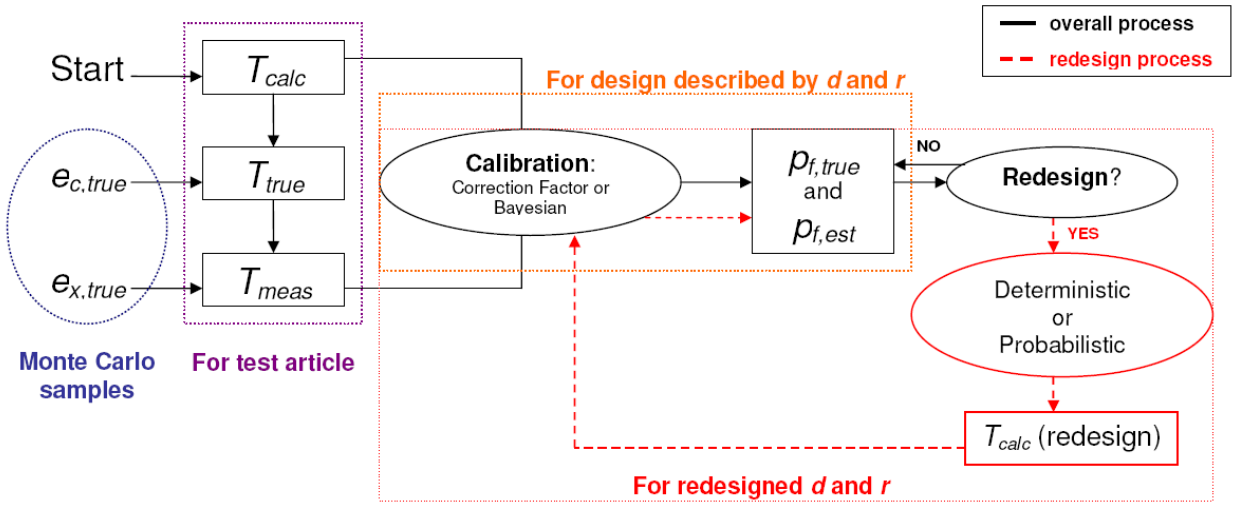

Figure 6. Flow chart highlighting the major processes involved in simulating one outcome of a future test. Note that a design can be redesigned only once.

To determine another possible outcome, the true computational and experimental errors are re-sampled and the process is repeated. Therefore, for n possible outcomes of a future test, we sample n pairs of the errors, have n true and estimated probabilities of failure after the test, and n number of designs after the test (if redesign is implemented, all designs will not be the same).

VI. Illustrative Example

In this example, we compare the probabilities of failure of an ITPS with the dimensions and material properties of probabilistic optimum found in Ref. 6. In that study, the optimum was found with constraints on the maximum bottom face sheet temperature, buckling of the web, and maximum von Mises stress in the webs with the bottom face sheet, web thickness, and foam thickness as the design variables. The failure considered here is exceeding the allowable bottom face sheet temperature T_{allow}. All random variables are normally distributed with the mean and coefficient of variation (CV) shown in Table 1.

Table 1. ITPS variables

Variable	Symbol	Nominal	CV (%)
bottom face sheet thickness	t_B	7.06 mm	2.89
foam thickness	d_S	71.3 mm	2.89
top face sheet thickness	t_T	1.2 mm	2.89
half unit cell length	p	34.1 mm	2.89
angle of corrugation	θ	80°	2.89
density of titanium	ρ_{Ti}	4429 kg/m^3	5.77
density of beryllium	ρ_{Be}	1850 kg/m^3	5.77
density of foam	ρ_S	24 kg/m^3	--
thermal conductivity of titanium	k_{Ti}	7.6 W/m/K	5.77
thermal conductivity of beryllium	k_{Be}	203 W/m/K	5.77
thermal conductivity of foam	k_S	0.105 W/m/K	5.77
specific heat of titanium	c_{Ti}	564 J/kg/K	5.77
specific heat of beryllium	c_{Be}	1875 J/kg/K	5.77
specific heat of foam	c_S	1120 J/kg/K	5.77

The distributions of e_c, and e_x are given below in Table 2. The original estimated probability of failure is 0.109% and the nominal mass per unit area is 35.1 kg/m^2.

Table 2. Distributions of error variables

Error	Distribution	Bounds
e_c	Uniform	±10%
e_x	Uniform	±3%

The extrapolation error e_{extrap} is calculated so that its value is 2% when d is at the ±10% bound of d_{test}.

$$e_{extrap} = 0.02\frac{|d - d_{test}|}{0.1 d_{test}} \tag{20}$$

In this example, we examine the benefits of including a future test by examining several cases that include future tests, one without redesign and one with redesign based on the future test by the process described in Sec. V. Using the procedure for calculating probabilities of failure with 1000 samples each of the response and capacity, we can compare these cases.

A. Future Test without Redesign

Considering 1000 possible outcomes of the single future test, the results in Table 3 were obtained. We observe that the mean true probability of failure is equal to that of the original estimated probability of failure before the test. This result is not unexpected as we did not allow redesign, thus preventing any changes in design and probability of failure.

Table 3. Results without including redesign

Parameter	Mean	Standard Deviation	Minimum	Maximum
$p_{f,true}$ (%)	0.109	0.374	0	2.00
$p_{f,est\text{-}corr}$ (%)	0.108	0.246	0	1.83

The corrected estimate obtained using the Bayesian approach does well at characterizing the true probability of failure after the future test. We observe that the corrected estimate slightly under predicts the true values, with the slightly smaller mean $p_{f,est\text{-}corr}$, standard deviation, and maximum value. With this approach, we would conclude that the design will be safer after the test.

B. Redesign Based on Test

In this example, we examine the effect of deterministic and probabilistic redesign. These two redesign methodologies are described in Section IV.

1. Deterministic Redesign

Deterministic redesign occurs when the $T_{meas}/T_{calc}(d_{test},r_{test})$ is greater than 1.05 (unconservative computational model), or when $T_{meas}/T_{calc}(d_{test},r_{test})$ is less than 0.95 (conservative computational model). We consider one design variable, the foam thickness d_s. This variable was chosen since it has a large impact on the bottom face sheet temperature.

The results including deterministic redesign are given in Table 4. Of the 1000 possible outcomes of the future test, 507 required redesign. Conservative cases account for 300 of the redesigns, and unconservative cases account for 207.

Table 4. Calibration by the correction factor approach with deterministic redesign

Parameter	Mean	Standard Deviation	Minimum	Maximum
m (kg/m^2)	34.9	2.8	28.9	41.4
d_s (mm)	70.4	12.1	44.9	98.5
$p_{f,true}$ (%)	0.0007	0.0083	0	0.1000

These results show that the true probability of failure is greatly reduced when redesign is allowed. In addition, the standard deviation is also reduced. Since the redesign is symmetric, it does not cause much change in the average mass[1]. The reason for this drastic reduction in probability of failure is the substantial reduction in error. So while the system was designed for a probability of failure of 0.1%, it ended up with a probability of failure of 0.0007%.

However, we note a large standard deviation in d_s, with the minimum and maximum values quite different from the design value of 71.3 mm. In practice, the redesign may not be allowed to be this drastic. Therefore, we also examine the case where the bounds of the redesigned d_s are restricted to ±10% of the original nominal d_s. These results are given in Table 5.

Table 5. Calibration by correction factor with deterministic redesign, bounds of redesigned d_s restricted to ±10% of d_{test}

Parameter	Mean	Standard Deviation	Minimum	Maximum
m (kg/m^2)	35.0	1.2	33.4	36.7
d_s (mm)	70.9	5.1	64.1	78.4
$p_{f,true}$ (%)	0.0007	0.0083	0	0.1000

[1] Mass per unit area before redesign is 35.1 kg/m^2

We observe that restricting the bounds of d_s does not change the true probability of failure, and does not cause a significant change in the average mass.

2. Probabilistic Redesign

The deterministic redesign reduced the average true probability of failure to 0.007% with and without bounds on the redesigned d_s. Using this result, we examine cases where the target redesign probability is $p_{f,target}$ = 0.01% with and without bounds on d_s. Here, we require redesign to occur when the estimated probability of failure $p_{f,est}$ is not within ±50% of the target, but reject the redesign if it does not decrease the mass by at least 4%. Since only one design variable, the foam thickness, is considered, a decrease in mass can only result from a decrease in foam thickness, which causes an increase in temperature. Therefore, the probability of failure can only be increased as a result of this redesign.

Of the 1000 possible outcomes of the future test, 598 are redesigned. Even with the requirement of a 4% decrease in mass, conservative models ($p_{f,est}$ less than target) account for all of the redesigns. This large number of conservative models is due to 718 of the 1000 cases having a $p_{f,est}$ of zero (due to the limited accuracy of the MC simulation) before the test. The results are shown in Table 6.

Table 6. Calibration by the Bayesian updating approach with probability of failure based redesign ($p_{f,target}$=0.01%)

Restriction on redesigned d_s	Parameter	Mean	Standard Deviation	Minimum	Maximum
No bounds	m (kg/m^2)	32.7	2.2	28.0	35.1
	d_s (mm)	61.2	9.6	41.0	71.3
	$p_{f,est\text{-}corr}$ (%)	0.474	1.126	0	10.77
	$p_{f,est\text{-}corr}$ (%) (no e_{extrap})	0.036	0.144	0	1.83
	$p_{f,true}$ (%)	0.035	0.195	0	1.83
Within ±10% of d_{test}	m (kg/m^2)	34.1	0.8	33.4	35.1
	d_s (mm)	67.0	3.5	64.1	71.3
	$p_{f,est\text{-}corr}$ (%)	0.034	0.145	0	1.83
	$p_{f,est\text{-}corr}$ (%) (no e_{extrap})	0.032	0.145	0	1.83
	$p_{f,true}$ (%)	0.032	0.195	0	1.83

Without bounds on the redesigned d_s, we observe that the true probability of failure is unable to converge to the target probability of failure of 0.01%, but we benefit from a significant reduction in mass and a reduction in the original mean true probability of failure from 0.109% to 0.035%. However, the estimated probability of failure, which includes the extrapolation error, leads us to believe that the design is made less safe overall. When this extrapolation error is not included, the estimated probability of failure provides a fairly accurate prediction of the true probability of failure, thus displaying the need to have reasonable bounds on the design variables to prevent large extrapolation errors.

When we include the bounds on d_s, the true probability of failure still does not converge to the target probability of failure, but there is better agreement between the estimated probabilities of failure (with and without the extrapolation error) and the true value. Due to the restricted bounds on d_s, the extrapolation error does not reach a value larger than 2%, which consequently prevents a gross overestimate of the probability of failure. We also note a 2.9% reduction in mass from the original value.

VII. Conclusion

This study presented a methodology to include the effect of a single future test followed by redesign on the probability of an integrated thermal protection system. Two ways of calibration and redesign based on the test were presented. We observed that the deterministic approach, which represents current design/redesign practices, leads to a greatly reduced probability of failure after the test and redesign, a reduction that usually is not quantified.

The probabilistic approach includes the Bayesian technique for calibrating the temperature calculation and re-design to a target probability of failure. It provides a way to accurately estimate the true probability of failure after the test. In addition, it allows us to trade weight against safety.

Future work includes incorporating the effect of the future test into the optimization of the ITPS. This study has brought to light many tunable parameters in the test, such as the bounds on the design variables, the target probability of failure for redesign, and the redesign criterion itself. By including these parameters into the optimization, we will not only optimize the design but optimize the test as well.

Acknowledgements

The material is based upon work supported by NASA under award No.NNX08AB40A. Any opinions, findings, and conclusions or recommendations expressed in this material are those of the author(s) and do not necessarily reflect the views of the National Aeronautics and Space Administration.

References

[1]Acar, E., Haftka, R.T., Kim, N.H., Buchi, D. "Effects of structural tests on aircraft safety," 50th AIAA/ASME/ASCE/AHS/ASC Structures, Structural Dynamics, and Materials Conference, Palm Springs, CA, May 2009

[2]Acar, E., Haftka, R.T., Kim, N.H., Buchi, D. "Including the Effects of Future Tests in Aircraft Structural Design," 8th World Congress for Structural and Multidisciplinary Optimization, Lisbon, Portugal, June 2009

[3]Kale, A., Haftka, R.T., "Tradeoff of Weight and Inspection Cost in Reliability-Based Structural Optimization," Journal of Aircraft, Vol. 45, No.1, 2008, pp. 77-85.

[4]Kale, A., Haftka, R.T., Sankar, B.V., "Efficient Reliability-Based Design and Inspection of Panels Against Fatigue," Journal of Aircraft, Vol. 45, No.1, 2008, pp. 86-96.

[5]Kumar. S., Villanueva, D., Sankar, B.V., Haftka, R.T., "Probabilistic Optimization of Integrated Thermal Protection Systems," AIAA-2008-5928, 12th AIAA/ISSMO Multidisciplinary Analysis and Optimization Conference, Victoria, British Columbia, Canada, September 2008

[6]Villanueva, D., Sharma, A., Haftka, R.T., Sankar, B.V., "Risk Allocation by Optimization of an Integrated Thermal Protection System," 8th World Congress for Structural and Multidisciplinary Optimization, Lisbon, Portugal, June 2009

[7]Bapanapalli, S.K., "Design of an Integrated Thermal Protection System for Future Space Vehicles," PhD Dissertation, University of Florida, 2007

[8]Smarslok, B.P., Haftka, R.T., and Kim, N.H. "Taking Advantage of Separable Limit States in Sampling Procedures," 47th AIAA/ASME/ASCE/AHS/ASC Structures, Structural Dynamics, and Materials Conference, Newport, RI, May 2006

[9]Oberkampf, W.L., Deland, S.M., Rutherford, B.M., Diegert, K.V., and Alvin, K.F., "Error and Uncertainty in Modeling and Simulation," Reliability Engineering and System Safety, Vol. 75, 2002, pp. 333-357.